A Relative Contact Formulation for Multibody System Dynamics

Byungok Roh
Department of Industrial Engineering, Sunmoon University
Hosung Aum
Department of Mechanical Engineering, Sunmoon University
Daesung Bae*, Heuije Cho
Department of Mechanical Engineering, Hanyang University
Hakyung Sung
Department of Precision Mechanical Engineering, Korea Electronic Technical Institute

Dynamic analysis of many mechanical systems is often involved with contacts among bodies. This paper presents a relative contact formulation for multibody dynamics in the context of the compliance contact model. Many conventional collision detection algorithms are based on the absolute coordinate system. This paper proposes to use the relative coordinate system in detecting a contact. A contact reference frame is defined on the defense body of a contact pair. Since all geometric variables necessary to detect a contact are measured relative to the contact reference frame attached to the defense body, the variables for a defense body are constant, which significantly reduces computation time. Therefore, the contact frame plays a key role in developing an efficient contact search algorithm. Contour of a defense body is approximated by many piecewise straight lines, while contour of a hitting body is represented by hitting nodes along its boundary. Bounding boxes containing each body of a contact pair are defined at a pre-search stage to eliminate the exhaustive contact inspection process when two bodies are in a distance. Domain of the bounding box for a defense body is divided into many sectors each of which has a list of line segments lying inside or on the sector boundary. Post-search for a contact is processed in the sequence of broad and narrow phases. In the broad phase, the bounding boxes of a contact pair are inspected for a contact. If two boxes are in a contact, each node on the hitting boundary is inspected to find out to which sector the node belongs. Since each domain sector of the defense body has a list of line segments, each node on the hitting boundary is tested for a contact only with the line segments in the list. In the narrow phase, actual contact calculation is carried out to find the contact penetration used in calculating the contact force. Since the searching algorithm is coupled with the stepping algorithm of the numerical integration, a strategy for deciding an integration stepsize is proposed. One numerical example is presented to demonstrate the validity of the proposed method.

Key Words : Multibody Dynamics, Contact Pairs, Contact Frame, Contact Calculation

1. Introduction

This paper presents a contact analysis algorithm employing the relative coordinate system for the multibody system dynamics. Multiple-contact higher pairs are widely used in mechanical systems such as walking machines, feeding systems, driving chains, and tracks of off-road vehicles.

* Corresponding Author,
E-mail : dsbae@email.hanyang.ac.kr
TEL : +82-31-400-5250
Department of Mechanical Engineering College of Engineering, Hanyang University Ansan, Kyunggido 425-791, Korea. (Manuscript **Received** February 3, 2000; **Revised** September 6, 2000)

Common design problems due to the multiple contacts among bodies are undercutting, jamming, backlash, and body interference.

The configuration space representation of a higher pair was proposed by Lozano-Perez (1983) for robot motion planning. Sacks(1998) extended the configuration space concept in for efficient detection of contact pairs. The relative position and orientation of a pair were mapped into the configuration space. The degrees of freedom of a pair became the dimension of the configuration space, which is divided into free space and contact space in the preprocessing stage of a dynamic analysis and is tabulated into a database. Run time query is made to decide whether a pair is currently in contact or not. When a higher pair has many degrees of freedom, formation of the configuration space and processing effort for a run time query may become extensive.

Wang(1999) presented an interference analysis method. Relative coordinates were defined for a contact pair and a kinematic closed loop including the contact pair was formed. Constraint equations arising from closed loops are solved for the relative coordinates including the ones for the contact pair. The canonical Hamiltonian formulation is used to derive a minimal set of dynamic equations of motion.

Mirtich(1996) proposed a contact detection algorithm consisting of narrow and broad phases. Candidate features are selected in the broad phase and contact inspection is carried out in the narrow phase only among the candidate features.

Haug(1986) presented a formulation for domains of mobility that characterizes kinematic boundaries of multiple contact pairs. A surface-surface contact joint was developed by Nelson (1998). Piecewise dynamic analysis method for a contact problem was employed. Dynamic analysis is halted when a contact pair is detected to be in contact and is resumed with new velocities that are calculated from the momentum balance equations. One of the drawbacks of this method is that too frequent halting and resuming of the numerical integration may occur when a contact pair toggles between contact and not contact states.

Zhong(1993) summarized many contact search algorithms in the area of finite element analysis. All geometric variables necessary to detect a contact was expressed in the absolute Cartesian coordinate system. The penalty and Lagrange multiplier methods were proposed. The compliant contact model that is based on the Herzian law was used by Lankarani(1992). Since the contact force is large and varies significantly, the differential equations of motion for this method are generally stiff.

This paper presents a hybrid contact detection algorithm of the configuration space method and bounding box method in conjunction with the compliant contact model. Two bodies of a contact pair are logically considered as a base body on which the contact reference frame is defined and as an action body which moves relative to the base body, respectively. Contour of the base body is approximated by many piecewise straight lines which are projected on axes of the contact reference frame. Each axis of the contact reference frame is divided into several segments each of which is indexed. Contact inspection for a contact pair is processed in the sequence of broad and narrow phases. Relative position vector of the action body to the base body is projected on the axes of the contact reference frame and selected candidate features that may come in contact shortly in the broad inspection phase, which greatly reduces the searching effort. No database needs to be built prior to the analysis. Since the searching algorithm is coupled with stepping algorithm of the numerical integration, a strategy for deciding a integration stepsize is proposed. A numerical example is presented to demonstrate the validity of the proposed method.

2. A contact Detection Method

2.1 Kinematic notations of a contact pair

Consider a contact pair shown in Fig. 1. Two bodies of the contact pair will be referred as a hitting body and a defense body, respectively, for convenience in the following discussions. The contours of the hitting and defense bodies will be referred to as the hitting and target boundaries, respectively. The X−Y−Z is the inertial referen-

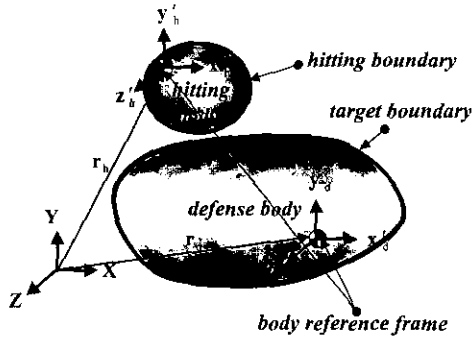

Fig. 1 A contact pair

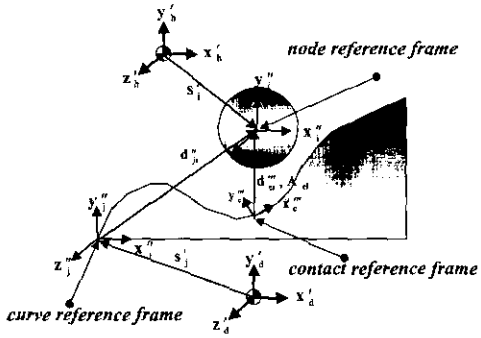

Fig. 2 Kinematics relationship of a contact pair

ce frame and primed coordinate systems are the body reference frames. The orientation and position of the body reference frame is denoted by $\mathbf{A}$ and $\mathbf{r}$, respectively. Double primed coordinate systems in Fig. 2 are the node reference frame of the hitting body and the curve reference frame of the defense body, respectively. In these coordinate systems, the nodes and line segments are in the same plane. Triple primed coordinate system is the contact reference frame of the defense body in detecting a contact, as shown in Fig. 2. The contact reference frame for the pair is defined on the defense body and the relative position and orientation of the hitting body to the defense body are defined as the generalized coordinates, which are denoted by $\mathbf{d}'''_{cl}$ and $\mathbf{A}_{cl}$, as shown in Fig. 2. Therefore, the generalized coordinates are directly used to detect a contact for the pair.

2.2 Division of the contact domain

Contour of a smoothly shaped body has been represented by the parametric B-spline curve many commercial CAD programs (Farvin, 1997).

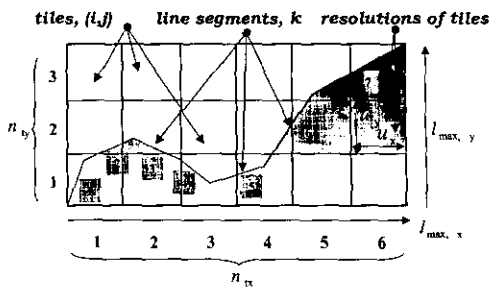

Fig. 3 Tile arrays and line segments

Since it is computationally extensive to find intersection points between two B-spline curves, segments of the B-spline curve are approximated by piecewise lines, as shown in Fig. 3. The domain of contact is divided into many tiles to efficiently process a contact detection, as shown in Fig. 3. The numbers of line segments and tiles which are denoted by n_l and $n_t = n_{tx} \times n_{ty}$ respectively. Their numbers will be decided by the degree of accuracy required. Once n_{tx} and n_{ty} are determined, then the resolutions of each tile denoted by u_x and u_y are determined.

In this paper, two arrays containg the information of line segments are used to efficiently process a contact search. The arrays will be referred as tile array and n-tile array. The size of the n-tile array equals to the number of tiles each of which contains the number of line segments in it. The size of the tile array equals to $n_t \times n_l$ and each of the array has the list of line segments in it. In Fig. 3, the sizes of the n-tile and the tile arrays are eighteen and one hundred twenty six, respectively. Minimum and maximum domain indices of the k th line segment can be obtained as follows.

$$i_1 = \frac{l''_{k1,x}}{u_x} + 1,\ i_2 = \frac{l''_{k2,x}}{u_x} + 1 \tag{1}$$

$$j_1 = \frac{l''_{k1,y}}{u_y} + 1,\ j_2 = \frac{l''_{k2,y}}{u_y} + 1 \tag{2}$$

where $l''_{k1,x}$, $l''_{k1,y}$, $l''_{k2,y}$ are the x and y components of vectors $\mathbf{l}''_{k1}$ and $\mathbf{l}''_{k2}$ shown in Fig. 4, respectively. If the i_2 and j_2 in Eqs. (1) and (2) are greater than n_{tx} and n_{ty}, then they are set by n_{tx} and n_{ty}, respectively. The algorithm in assembling the n-tile and tile arrays is represented as follows.

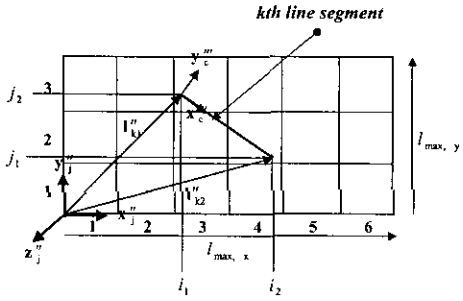

Fig. 4 Line segments and assemble tile arrays

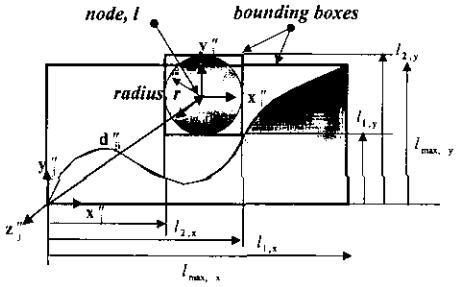

Fig. 5 Bounding boxes

```
do k=1, n_l
  compute i_1, i_2, j_1 and j_2 from eqs. (1)
  and (2)
  do i=i_1, i_2
    do j=j_1, j_2
      ntile(i, j)=ntile(i, j)+1
      tile(ntile(i, j), i, j)=k
    enddo
  enddo
enddo
```

If the global coordinate system were adopted, formation process of the tile and n-tile arrays would become very expensive because the process must be repeated at every time step. However, the proposed method employs the relative contact formulation which yields the constant tile and n-tile arrays. This saves the computation time significantly.

2.3 Pre-search

In order to detect a contact between two boundaries of a contact pair, every pair of the nodes on the hitting boundary and the lines on the target boundary must be examined, which is computationally extensive. Bounding boxes are defined to save the exhaustive examination at the pre-search stage such that their edges are parallel to the coordinate axes of the double primed reference frame attached to each body, as shown in Fig. 5. The boxes must completely contain all boundary nodes and lines of the hitting and defense bodies. In this step, it is determined whether the nodes of the hitting body are inside of the bounding box of the defese body. The relative positions of the nodes to the curve reference frame shown in Figs. 1 and 2 can be obtained as follows.

$$\mathbf{d}_{jl}=\mathbf{r}_h+\mathbf{s}_i-\mathbf{r}_d+\mathbf{s}_j \tag{3}$$

The $\mathbf{d}_{jl}$ vector in Eq. (3) in the curve reference frame is obtained as

$$\mathbf{d}''_{jl}=\mathbf{A}^T_{dj}\,\mathbf{d}_{jl} \tag{4}$$

where $\mathbf{A}_{dj}=\mathbf{A}_d\,\mathbf{C}_j$ and $\mathbf{C}_j$ is the orientation matrix of the curve reference frame with respect to the defense body reference frame. Thus, indices of the bounding box of the lth node are determined as follows.

$$i_1=\frac{(\mathbf{d}''_{jl,x}-r)}{u_x}+1,\ i_1=\frac{(\mathbf{d}''_{jl,x}+r)}{u_x}+1 \tag{5}$$

$$j_1=\frac{(\mathbf{d}''_{jl,y}-r)}{u_y}+1,\ j_1=\frac{(\mathbf{d}''_{jl,y}+r)}{u_y}+1 \tag{6}$$

where r is the radius of the node. The $\mathbf{d}''_{jl,x}$ and $\mathbf{d}''_{jl,y}$ are the x and y components of the vector $\mathbf{d}''_{jl}$ shown in Fig. 2. If i_1 is greater than n_{tx} or i_2 is less than 0, then the contact pair is in the non-contact state. If j_1 is greater than n_{ty} or j_2 is less than 0, then the contact pair is also in the non-contact state. If the pair is not in non-contact state, then post-search step will be proceeded.

2.4 Broad phase of the post-search

Prior to an extensive contact examination, two bounding boxes for the defense and hitting bodies have been tested for a contact. Domain of the box for the defense body is divided into many tiles, as shown in Fig. 6. Each tile has a set of line segments lying within or on the tile boundary. If the bounding boxes of nodes are turned out to be in a contact, the next step which is referred as a broad phase is to find candidate line segments for each node in the hitting body.

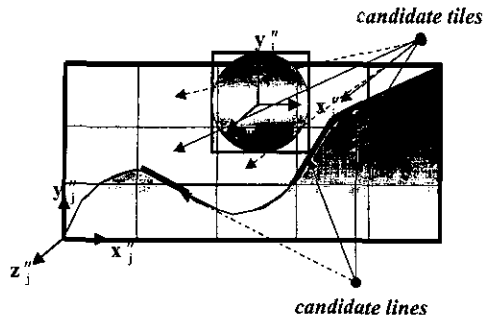

Fig. 6 Concept in broad phase

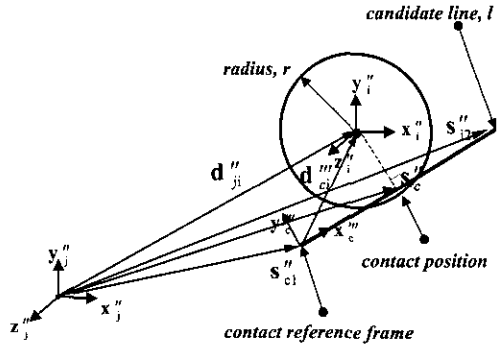

Fig. 7 Concept in narrow phase

The candidate line segments can be found by using the *tile* and *n-tile* arrays. Candidate *tiles* containing the numbers and list of candidate lines are determined by the indices of each node calculated from Eqs. (5) and (6). Thus, no further inspection is carried out for the non-candidate nodes.

2.5 Narrow phase of the post-search and compliant contact force

The candidate line segments on the target boundary have been selected for each node on the hitting boundary in the broad phase. In this step, each node in bounding box contacting with the line segments is inspected if it is in a contact. The nodal position vector $\mathbf{d}''_{ci}$ is obtained by Eq. (4) and Fig. 7 as follows.

$$\mathbf{d}''_{ci}=\mathbf{d}''_{ji}-\mathbf{s}''_{ci} \tag{7}$$

The vector $\mathbf{d}'''_{ci}$ in the contact reference frame is obtained as

$$\mathbf{d}'''_{ci}=\mathbf{C}^{T}_{c}\,\mathbf{d}''_{ci} \tag{8}$$

where $\mathbf{C}_c$ is the orientation matrix of the contact reference frame with respect to the curve reference frame.

The first contact condition is that the x component of the vector $\mathbf{d}'''_{ci}$ is greater than $-r$ and less than l_c+r. The l_c is obtained by

$$l_c=\mathbf{f}^{T}\,\mathbf{C}^{T}_{c}(\mathbf{s}''_{c2}-\mathbf{s}''_{c1}) \tag{9}$$

where $\mathbf{f}=\{1, 0, 0\}^T$. The second contact condition is that the penetration of the node into the line segment is greater than zero. The penetration of the node into the line segment is calculated by

$$\delta=r-\mathbf{h}^{T}\,\mathbf{d}'''_{ci} \tag{10}$$

where $\mathbf{h}=\{0, 0, 1\}^T$. If both contact conditions are satisfied, the contact position vector in the curve reference frame can be obtained as follows.

$$\mathbf{s}_c=\mathbf{s}''_{c1}+\mathbf{C}_c\,\mathbf{f}\,\mathbf{d}'''_{ci} \tag{11}$$

Thus, the contact force is obtained by

$$\mathbf{f}_c=-k\delta-c\dot{\delta} \tag{12}$$

where k and c are the spring and damping coefficient respectively, which are determined by experimental method $\dot{\delta}$ is the time differentiation of δ.

3. Kinematics and Equations of Motion for the Recursive Formulas

A contact search algorithm is proposed in Sect. 2. The proposed method makes use of the relative position and orientation matrix for a contact pair. This section presents the relative coordinate kinematics for a contact pair as well as for joints connecting two bodies. Translational and angular velocities of the $x_i'-y_i'-z_i'$ frame in the $X-Y-Z$ frame are respectively defined as $\dot{\mathbf{r}}_i$ and $\boldsymbol{\omega}_i$. Their corresponding quantities in the $x_i'-y_i'-z_i'$ frame are defined as

$$\mathbf{Y}_i\equiv\begin{bmatrix}\dot{\mathbf{r}}_i'\\ \boldsymbol{\omega}_i'\end{bmatrix}=\begin{bmatrix}\mathbf{A}_i^{T}\dot{\mathbf{r}}_i\\ \mathbf{A}_i^{T}\boldsymbol{\omega}_i\end{bmatrix} \tag{13}$$

where $\mathbf{Y}_i$ is the combined velocity of translation and rotation. A tilde operator associated with vectors $\mathbf{a}$ and $\mathbf{b}$ to denote the vector cross product is defined as follows.

$$\tilde{\mathbf{a}}\mathbf{b}=\mathbf{a}\times\mathbf{b}$$

Recursive velocity formula for a pair of contiguous bodies have been derived by Angeles (1997) and Lee etal (1994) as follows

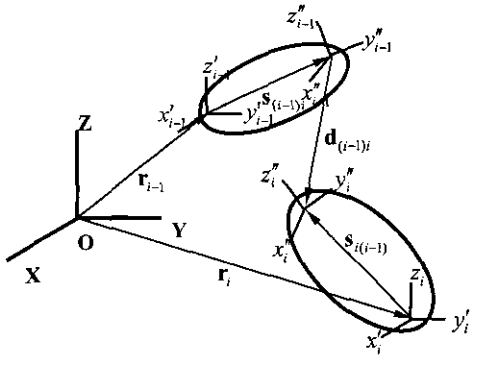

Fig. 8 Kinematics relationship between two adjacent rigid bodies

$$\mathbf{Y}_i=\mathbf{B}_{(i-1)i1}\mathbf{Y}_{(i-1)}+\mathbf{B}_{(i-1)i2}\mathbf{v}_{(i-1)i} \tag{14}$$

where $\mathbf{v}_{(i-1)i}$ denotes the relative velocity vector for joint $(i-1)i$ and the matrices $\mathbf{B}_{(i-1)i1}$ and $\mathbf{B}_{(i-1)i2}$ are

$$\mathbf{B}_{(i-1)i1}=\begin{bmatrix}\mathbf{A}_{(i-1)i}^{\mathrm{T}} & 0\\ 0 & \mathbf{A}_{(i-1)i}^{\mathrm{T}}\end{bmatrix}\begin{bmatrix}\mathbf{I} & -(\tilde{\mathbf{s}}'_{(i-1)i}+\tilde{\mathbf{d}}'_{(i-1)i}-\mathbf{A}_{(i-1)i}\tilde{\mathbf{s}}'_{(i-1)i}\mathbf{A}_{(i-1)i}^{\mathrm{T}})\\ 0 & \mathbf{I}\end{bmatrix}$$

$$\mathbf{B}_{(i-1)i2}=\begin{bmatrix}\mathbf{A}_{(i-1)i}^{\mathrm{T}} & 0\\ 0 & \mathbf{A}_{(i-1)i}^{\mathrm{T}}\end{bmatrix}\begin{bmatrix}(\mathbf{d}'_{(i-1)i})_{\mathbf{q}(i-1)i}+\mathbf{A}_{(i-1)i}\tilde{\mathbf{s}}'_{(i-1)i}\mathbf{A}_{(i-1)i}^{\mathrm{T}}\mathbf{H}'_{(i-1)i}\\ \mathbf{H}'_{(i-1)i}\end{bmatrix} \tag{15}$$

where $\mathbf{A}_{(i-1)i}^{\mathrm{T}}=\mathbf{A}_{(i-1)}^{\mathrm{T}}\mathbf{A}_i$, $\mathbf{s}'_{(i-1)i}=\mathbf{A}_{(i-1)}^{\mathrm{T}}\mathbf{s}_{(i-1)i}$, $\mathbf{d}'_{(i-1)i}=\mathbf{A}_{(i-1)}^{\mathrm{T}}\mathbf{d}_{(i-1)i}$, $\mathbf{s}'_{(i-1)}=\mathbf{A}_i^{\mathrm{T}}\mathbf{s}_{(i-1)i}$, and $(\mathbf{d}'_{(i-1)i})_{\mathbf{q}(i-1)i}=\partial\mathbf{d}'_{(i-1)i}/\partial\mathbf{q}_{(i-1)i}$. The matrix $\mathbf{H}'_{(i-1)i}$ is determined by the axis of rotation and $\mathbf{q}_{(i-1)i}$ denotes the relative generalized coordinate vector for joint $(i-1)i$. The vectors $\mathbf{s}'_{(i-1)i}$ and $\mathbf{s}'_{(i-1)i}$ are defined in Fig. 8. Also, the virtual displacement in the Cartesian coordinate and relative coordinate systems has been shown to have the following relationship:

$$\delta\mathbf{Z}=\mathbf{B}\delta\mathbf{q} \tag{16}$$

where $\delta\mathbf{Z}$ must be kinematically admissible for all joints for a tree structure consisting of n serial bodies.

The virtual work done by a Cartesian force $\mathbf{Q}\in\mathbf{R}^{nc}$ where nc is the number of Cartesian coordinatesis is obtained as follows.

$$\delta\mathrm{W}=\delta\mathbf{Z}^{\mathrm{T}}\mathbf{Q} \tag{17}$$

Substitution of Eq. (16) into Eq. (17) yields

$$\delta\mathrm{W}=\delta\mathbf{q}^{\mathrm{T}}\mathbf{B}^{\mathrm{T}}\mathbf{Q}=\delta\mathbf{q}^{\mathrm{T}}\mathbf{Q}^{*} \tag{18}$$

where $\mathbf{Q}^{*}=\mathbf{B}^{\mathrm{T}}\mathbf{Q}$.

The variational form of the equations of motion for constrained mechanical systems is

$$\delta\mathbf{q}^{\mathrm{T}}\{\mathbf{B}^{\mathrm{T}}(\mathbf{M}\dot{\mathbf{Y}}+\boldsymbol{\Phi}_z^{\mathrm{T}}\boldsymbol{\lambda}-\mathbf{Q})\}=0 \tag{19}$$

where $\delta\mathbf{q}$ must be kinematically admissible for all tree structure joints, $\boldsymbol{\lambda}\in\mathbf{R}^{m}$ is the Lagrange multiplier vector for cut joints (Wittenburg, 1977) and m is the number of cut constraints. $\boldsymbol{\Phi}\in\mathbf{R}^{m}$ and $\boldsymbol{\Phi}_z$ represent the position-level constraint vector and the constraint Jacobian matrix, respectively. The mass matrix $\mathbf{M}$ and the force vector $\mathbf{Q}$ are defined as follow.

$$\mathbf{M}=\mathrm{diag}(\mathbf{M}_1,\ \mathbf{M}_2,\ \cdots,\ \mathbf{M}_{\mathrm{nbd}}) \tag{20}$$

$$\mathbf{Q}=(\mathbf{Q}_1^{\mathrm{T}},\ \mathbf{Q}_2^{\mathrm{T}},\ \cdots,\ \mathbf{Q}_{\mathrm{nbd}}^{\mathrm{T}})^{\mathrm{T}} \tag{21}$$

where nbd denotes the number of bodies. Since $\delta\mathbf{q}$ is arbitrary, the following equations of motion are obtained.

$$\mathbf{F}=\mathbf{B}^{\mathrm{T}}(\mathbf{M}\dot{\mathbf{Y}}+\boldsymbol{\Phi}_z^{\mathrm{T}}\boldsymbol{\lambda}-\mathbf{Q})=0 \tag{22}$$

The equations of motion and the position level constraint can be implicitly rewritten by introducing $\mathbf{v}\equiv\dot{\mathbf{q}}$ as

$$\mathbf{F}(\mathbf{q},\ \mathbf{v},\ \dot{\mathbf{v}},\ \boldsymbol{\lambda})=0 \tag{23}$$

$$\boldsymbol{\Phi}(\mathbf{q})=0 \tag{24}$$

Successive differentiations of the position level constraint yield

$$\dot{\boldsymbol{\Phi}}(\mathbf{q},\ \mathbf{v})=\boldsymbol{\Phi}_{\mathrm{p}}\mathbf{v}-\nu=0 \tag{25}$$

$$\ddot{\boldsymbol{\Phi}}(\mathbf{q},\ \mathbf{v},\ \dot{\mathbf{v}})=\boldsymbol{\Phi}_{\mathrm{p}}\dot{\mathbf{v}}-\gamma=0 \tag{26}$$

Eq. (23) and all levels of constraints comprise the overdetermined differential algebraic system (ODAS). An algorithm for the backward differentiation formula (BDF) to solve the ODAS is given by Yen et al (1990) as follows.

$$\mathbf{H}(\mathbf{p})=\begin{bmatrix}\mathbf{F}(\mathbf{p})\\ \dot{\boldsymbol{\Phi}}\\ \boldsymbol{\Phi}\\ \mathbf{U}_0^{\mathrm{T}}(\frac{h}{b_0}\mathbf{R}_1)\\ \mathbf{U}_0^{\mathrm{T}}(\frac{h}{b_0}\mathbf{R}_2)\end{bmatrix}=\begin{bmatrix}\mathbf{F}(\mathbf{q},\ \mathbf{v},\ \dot{\mathbf{v}},\ \boldsymbol{\lambda})\\ \boldsymbol{\Phi}_{\mathrm{q}}\dot{\mathbf{v}}-\gamma\\ \boldsymbol{\Phi}_{\mathrm{q}}\mathbf{v}-\nu\\ \boldsymbol{\Phi}(\mathbf{q})\\ \mathbf{U}_0^{\mathrm{T}}(\frac{h}{b_0}\dot{\mathbf{v}}-\mathbf{v}-\zeta_1)\\ \mathbf{U}_0^{\mathrm{T}}(\frac{h}{b_0}\mathbf{v}-\mathbf{q}-\zeta_2)\end{bmatrix}=0 \tag{27}$$

where $\zeta_1\equiv\frac{1}{b_0}\sum_{i=1}^{k}b_i\mathbf{v}_{(-i)}$ and $\zeta_2\equiv\frac{1}{b_0}\sum_{i=1}^{k}b_i\mathbf{q}_{(-i)}$, in which k is the order of integration, b_is are the BDF coefficients $\mathbf{p}\equiv[\mathbf{q}^{\mathrm{T}},\ \mathbf{v}^{\mathrm{T}},\ \dot{\mathbf{v}}^{\mathrm{T}},\ \boldsymbol{\lambda}^{\mathrm{T}}]^{\mathrm{T}}$. The col-

umns of $U_0 \in R^{nr\times(nr-m)}$ constitute the bases for the parameter space of the position-level constraints and are obtained by LU-decomposition of the constraint Jacobian so that the following matrix is nonsingular:

$$\begin{bmatrix} \Phi_q \\ U_0^T \end{bmatrix} \tag{28}$$

The number of equations and the number of unknowns in Eq. (27) are the same, and so Eq. (27) can be solved for $\mathbf{p}$. Newton Raphson method can be applied to obtain the solution $\mathbf{p}$.

$$\mathbf{H}_p \Delta\mathbf{p} = -\mathbf{H} \tag{29}$$

$$\mathbf{p}^{i+1} = \mathbf{p}^i + \Delta\mathbf{p} \tag{30}$$

where

$$\mathbf{H}_p = \begin{bmatrix} \mathbf{F}_q & \mathbf{F}_v & \mathbf{F}_t & \mathbf{F}_\lambda \\ \Phi_q & 0 & 0 & 0 \\ \dot{\Phi}_q & \dot{\Phi}_v & 0 & 0 \\ \ddot{\Phi}_q & \ddot{\Phi}_v & \ddot{\Phi}_t & 0 \\ U_0^T & \beta_0 U_0^T & 0 & 0 \\ 0 & U_0^T & \beta_0 U_0^T & 0 \end{bmatrix} \tag{31}$$

Recursive formulas for $\mathbf{H}_p$ and $\mathbf{H}$ in Eq. (29) are derived to evaluate them efficiently.

4. Numerical Integration Strategy

The sufficient condition for a successful numerical integration step is to satisfy both accuracy and stability of the state variables for a system without a contact. Satisfaction of the accuracy and stability is not sufficient for a system with a contact. Suppose a bullet collides with an object. If the object is thin, the bullet passes through the object without noticing it. If the object is thick and a moderately large step size satisfies both the accuracy and stability, the bullet penetrates too deep at the first step of a contact. Large and sudden contact force due to large penetration generally introduces a large numerical error in the state variables. The large numerical error often causes the integration step to fail. Therefore, the contact condition must be considered in deciding an integration step.

In order to make a system transition from a non-contact status to a contact status as smooth as possible, the time of contact must be predicted accurately. However, the computationally extensive search algorithm must be triggered to predict the exact time of contact even though the two bodies of a contact pair are located at a distance. Easy and practical solution to this problem is to use the method of backtracking. This paper adopted the concept of buffer radius shown in Fig. 9. In a narrow phase, if nodes with radius r in the hitting body are not contacted with the candidate lines in the defense body and not some nodes with buffer radius r_b are contacted, the integrating step will be decreased.

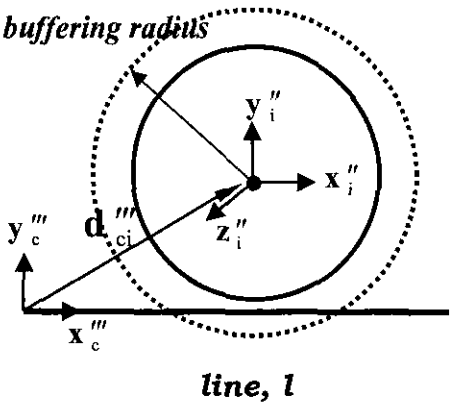

Fig. 9 A buffering radius of node

5. Numerical Example

The proposed algorithm is implemented in the commercial program **RecurDyn**. A wire wrapping system is solved to demonstrate the effectiveness of the proposed algorithm. It consists of two rollers and a wire as shown in Fig. 10. The wire is modeled as a series of 96 rigid nodes connected by revolute joints. The mass and inertia moment of nodes are 0.01kg and 0.05kg-m^2, respectively. The system has 99 degrees of freedom. The wire mainly carries tension with little torsion which is modeled by a torsional spring. Contact is defined between each string node and two rollers. The tensions and contact forces in some positions of the wire are shown in Fig. 11 and Fig. 12, respectively, while one end-position of the wire is pulled at a constant speed of 2m/sec and the other end-position of the wire is loaded with 196.13N. The spring and damping coefficients of each

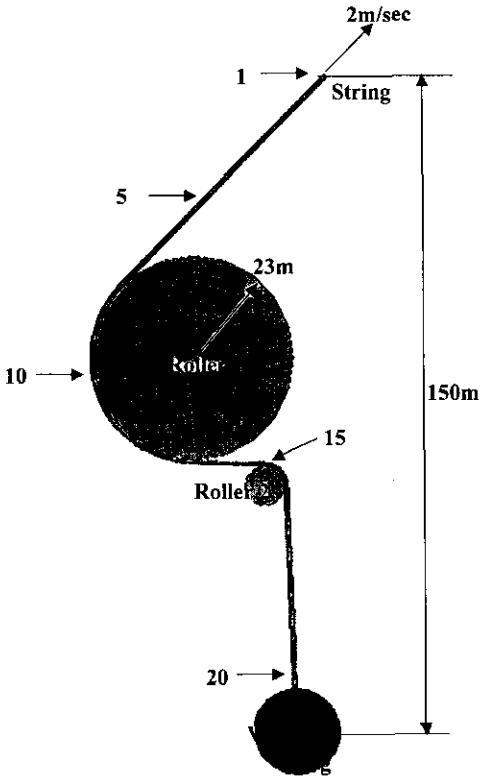

Fig. 10 A wire system

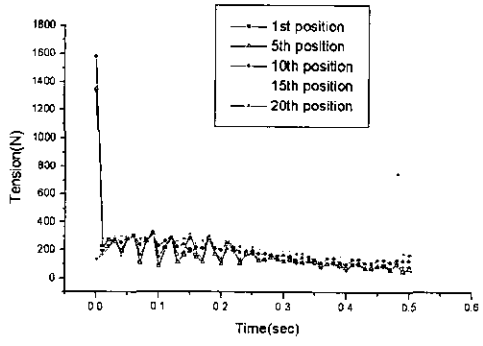

Fig. 11 Tensions in the positions 1, 5, 10, 15 and 20

contact force are 1000N/m and 100N-sec/m, respectively. The analysis was performed on a IBM compatible computer (Pentium Ⅲ -500Mhz) and took about 80 sec. for simulation.

6. Conclusions

This research proposes an efficient implementation algorithm for contact mechanisms. The con-

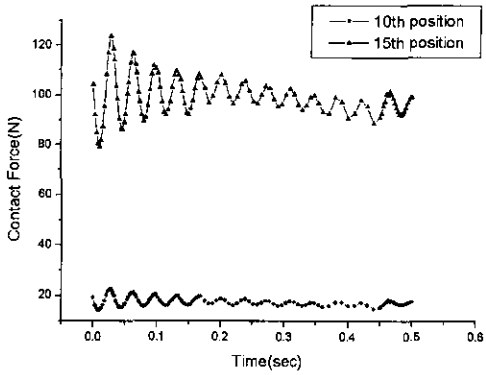

Fig. 12 Contact forces in the positions 10 and 15

tact domain is divided into many tiles each of which contains the list of lines inside it. The search process consists of pre-search and post search states. The post search process is again divided into broad and narrow phases. In the pre-search stage, the bounding box technique is employed to find an approximate contact state. Once the contact is detected in the pre-search stage, the detailed contact condition is further examined in the post-search stage. The compliance contact model is used to generate the contact force which is applied to the hitting and defense bodies. The relative coordinate formulation is used to generate the equations of motion. The local parametrization method is used to solve the differential algebraic equations. The integration stepsize is automatically reduced when a contact is expected to occur soon. The proposed algorithm is implemented in the commercial program **Recurdyn** and the wire system having fifty bodies and fifty revolute joints is successfully solved to predict the wire tension, while the wire is wrapping the roller.

References

Angeles, J., 1997, "Fundamentals of Robotic Mechanical Systems," Springer.

Farin, G., 1997, "Curves and Surfaces for Computer-aided Geometic Design," Academic Press.

Haug, E. J., Wu, S. C. and Yang, S. M., 1986, "Dynamic mechanical systems with Coulomb friction, stiction, impact and constraint addition-

deletion, I: Theory," *Mech. Mach. Theory*, Vol. 21(5), pp. 407~416.

Lankarani, H. M., 1992, "Canonical Impulse-Momentum Equations for Impact Analysis of Multibody System," ASME, *Journal of Mechanical Design*, Vol. 180, pp. 180~186.

Lee, D. C., Bae, D. S. and Han, C. S., 1994, "A Study on the Dynamic Analysis of Multibody System by the Relative Joint Coordinate Method," KSME, *Journal of the Korean Society of Mechanical Engineers*, Vol. 18, No. 8, pp. 1974~1984.

Lozano-Peñez, T., 1983, "Spatial Planning: A Configuration Space Approach," *IEEE Transactions on Computers*, Vol. C-32, IEEE Press.

Mirtich, B. V., 1996, "Impulse-based Dynamic Simulation of Rigid Body Sysyems," Ph. D thesis, University of California, Berkeley.

Nelson, D. D. and Cohen, E. 1998, "User Interaction with CAD Models with Non-holonomic Parametric Surface Constraints," *Proceedings of the ASME Dynamic Systems and Control Division*, DSC-Vol. 64, pp. 235~242.

Sacks, E. and Joskowicz, L., 1998, "Dynamical Simulation of Planar Systems with Changing Contacts Using Configuration Spaces," *Journal of Mechanical Design*, Vol. 120, pp. 181~187.

Wang, D., 1996, "A Computer-aided Kinematics and Dynamics of Multibody Systems with Contact Joints," Ph. D Thesis, Mons Polytechnic University Belgium.

Wang, D., Conti, C. and Beale, D., 1999, "Interference Impact Analysis of Multibody Systems," *Journal of Mechanical Design*, Vol. 121, pp. 121~135.

Wang, D., Conti, C., Dehombreux, P. and Verlinden, O., 1997, "A Computer-aided Simulation Approach for Mechanisms with Time-Varying Topology," *Computers and Structures*, Vol. 64, pp. 519~530.

Wittenburg, J., 1977, "Dynamics of Systems of Rigid Bodies," B. G. Teubner, Stuttgart.

Yen, J., Haug, E. J. and Potra, F. A., 1990, "Numerical Method for Constrained Equations of Motion in Mechanical Systems Dynamics," Technical Report R-92, Center for Simulation and Design Optimization, Department of Mechanical Engineering, and Department of Mathematics, University of Iowa, Iowa City, Iowa.

Zhong, Z. Z., 1993, "Finite Element Procedures for Contact-Impact Problems," Oxford University Press.